FABRICATION, CALIBRATION AND CHARACTERIZATION OF MICRO-SCALE RESISTANCE TEMPERATURE DETECTORS

by

KUNJAN ANILKUMAR CHAUDHARI

Presented to the Faculty of the Graduate School of

The University of Texas at Arlington in Partial Fulfillment

of the Requirements

for the Degree of

MASTER OF SCIENCE IN MECHANICAL ENGINEERING

THE UNIVERSITY OF TEXAS AT ARLINGTON

December 2016

Acknowledgements

I am honored to have got the opportunity to work under the guidance of Dr. Hyejin Moon who has been my pillar of support throughout my Master's Thesis at University of Texas at Arlington and for which I'm grateful to her. During this period, I have learned a lot about Micro-Scale temperature detectors and its application in Digital Microfluidics system.

I am grateful to Shreyas Bindiganavale whose research work on hotspot cooling of Integrated Circuits using EWOD Digital Microfluidics has helped me create the foundation of my work and I've learnt a great deal from his work.

I would like to thank my lab mates Arvind Venkatesan, Ali Farzbod, Shubhodeep Paul, Munmun Nahar and others for being there whenever I needed them and giving me valuable feedback and suggestions all throughout my thesis. I am obliged to engineers from NanoFAB lab, UTA for their guidance and training in using machineries involved in Microfabrication.

I would also like to express sincere gratitude to my all my friends who, directly or indirectly, have lent their helping hand in my venture.

None of my journey till here could have been possible if it weren't for the blessings and unconditional support of my parents and my family. They are the backbone of my life and I am blessed to have them.

November 17, 2016

Abstract

FABRICATION, CALIBRATION AND CHARACTERIZATION OF MICRO-SCALE RESISTANCE TEMPERATURE DETECTORS

Kunjan Anilkumar Chaudhari, MS

The University of Texas at Arlington, 2016

Supervising Professor: Hyejin Moon

Through this research, fabrication, calibration and characterization of micro-scale Resistance Temperature Detector (RTD) were studied. The RTD is meant to sense the temperature at the micro scale level on the hot spot of integrated circuit devices. Material that we focused in this study was indium tin oxide (ITO). Indium tin oxide thin films are widely used as an electrode owing to its optically transparent and electrical conducting properties. However, ITO thin film behavior as an RTD has not been well studied yet, which we aimed in this study. The commercially available ITO thin film deposited on a glass substrate was used in all the experiments. In addition, nickel which has a very linear temperature v/s resistance characteristic was also fabricated for comparison purpose. Nickel and ITO resistors were fabricated by standard microfabrication processes. Oil bath calibration process was implemented to maintain steady state temperature. The effect of annealing on the change in resistance of both ITO and nickel was studied. Experiments were carried out in different temperature ranges to validate the data. The study concludes that ITO thin film can be used as an RTD in a limited temperature range and its performance is highly affected by crystalline structure of ITO thin film layer.

Table of Contents

List of Illustrations

List of Tables

Chapter 1

INTRODUCTION

1.1 Motivation

The idea of fabricating, calibrating and characterizing a micro-scale resistive temperature detector (RTD) came from the previous studies which were carried out in the area of hotspot cooling of integrated circuit devices. It was observed that not only metals possess good resistance v/s temperature characteristics but certain semi-conductors also have similar linear characteristics over a limited range of temperature. The semi-conductor used in this study is indium tin oxide (ITO), a well-known transparent oxide thin film. Due to its high optical transmittance in the visible and near infrared regions, it has been widely applied in various optoelectronic devices, infrared reflectors, and display devices. Shreyas et al. [1] used ITO heater in the area of hotspot cooling for Integrated circuits using electrowetting on dielectric (EWOD) digital microfluidic system. The ITO heater/RTD solved the purpose of both emulating the hotspot and also measuring the temperature of the droplet. Moreover, ITO provides optical transparency without sacrificing other functions and is also an ideal material for EWOD patterning [1].

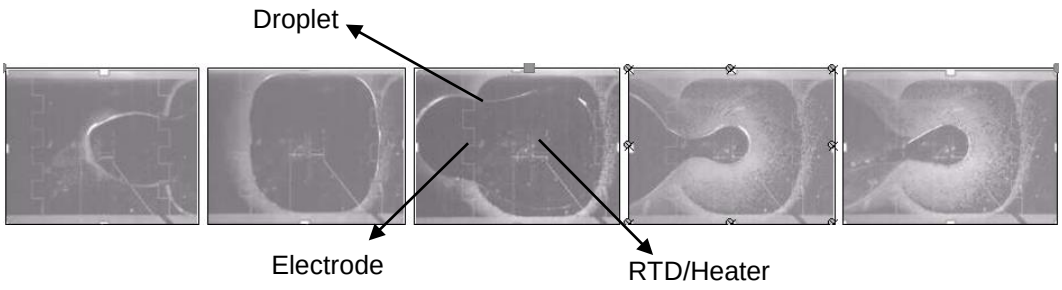

Figure 1-1 Figure showing ITO RTD/heater and EWOD setup [1]

The ITO heater/RTD was fabricated using thin film semiconductor fabrication techniques. The device was then calibrated using oil bath calibration technique. After calibration, it was observed that ITO showed linear positive temperature coefficient (PTC) characteristics over a certain range of temperature as shown in the Figure 1-2. This observation of ITO showing linear resistance v/s temperature plot inspired the research study to know exactly how the ITO behaves under various temperatures and also to know the limitation of ITO behavior as resistance temperature detector. In addition to that, the research also focusses on developing an alternative to the conventional temperature measuring sensors.

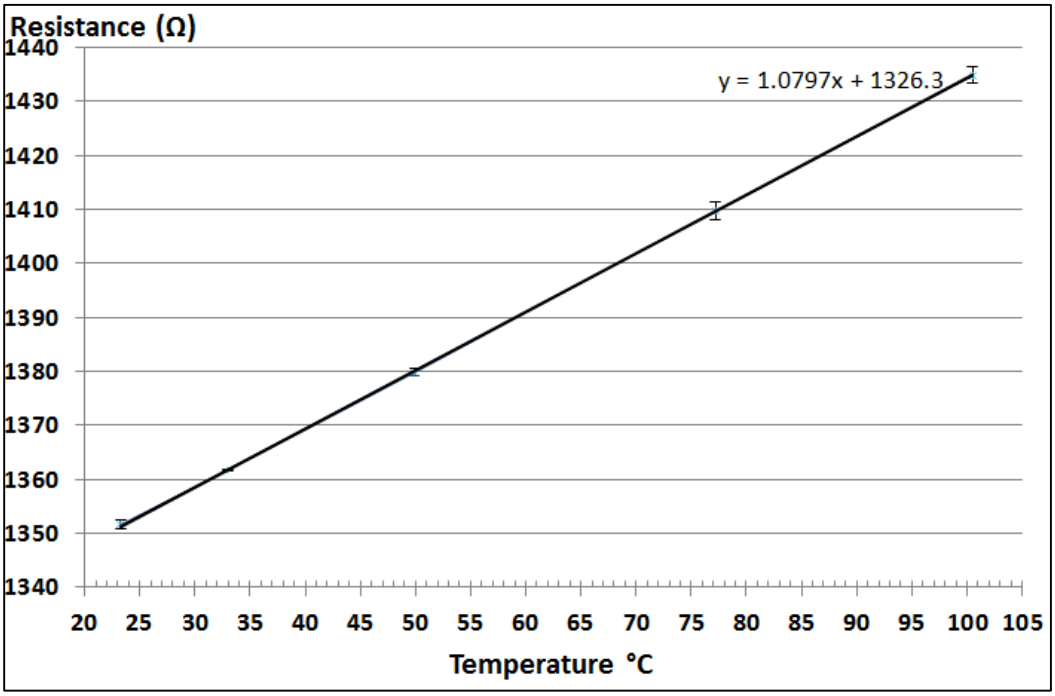

Figure 1-2 Data showing Calibration of ITO RTD [1]

1.2 Resistance Temperature Detectors(RTD):

Resistance temperature detectors are temperature sensors that contain a resistor that changes resistance value as its temperature changes. The change of resistance with temperature can be measured by common resistance measuring methods and it can be used to determine the temperature of a process or a material. Common RTD sensing elements constructed of platinum, copper or nickel have a repeatable resistance v/s temperature relationship (*R* vs *T*) in their operating temperature range. The resistance Vs temperature relationship is defined as the amount of resistance change of the sensor per degree of temperature change of the process. Most conductive materials change specific resistance with changes in temperature. This is why figures of specific resistance are always specified at a standard temperature (usually 20˚C or 25˚C).

The change in resistance factor per unit of temperature change is called the *temperature coefficient of resistance*. This factor is represented by the Greek lower-case letter “alpha” (α).

A positive coefficient for a material indicates that its resistance increases with an increase in temperature. Pure metals typically have positive temperature coefficients of resistance. Coefficients approaching zero can be obtained by alloying certain metals. The formula used to determine the resistance of a conductor at some temperature other than what is specified in a resistance table is as follows:

$R=R_{ref}[1+\alpha(T-T_{ref})]$

Where,

R=Resistance at temperature “T”.

R_{ref} = Resistance at reference temperature (usually 21˚C)

α = Temperature coefficient of resistivity for the sensor.

T=Unknown temperature to be measured.

T_{ref}=Reference temperature taken (21˚C).

Resistance thermometers have been used for many years to measure temperature in the laboratory and industrial processes, and have developed a reputation for accuracy, repeatability, and stability. RTDs are generally considered to be among the most accurate temperature sensors available. In addition to offering very good accuracy, RTD also provide excellent stability and repeatability. RTDs also feature high immunity to electrical noise and are, therefore, well suited for applications in process and industrial automation environments, especially around motors, generators, and other high voltage equipment.

RTD sensing elements come in two basic styles, wire wound, and thin film.

Wire wound elements contain a length of very small diameter wire (typically .0005 to .0015-inch diameter) which is either wound into a coil and packaged inside a ceramic mandrel or wound around the outside of a ceramic housing and coated with an insulating material. Larger lead wires (typically .008 to .015-inch diameter) are provided which allow the larger extension wires to be connected to the very small element wire.

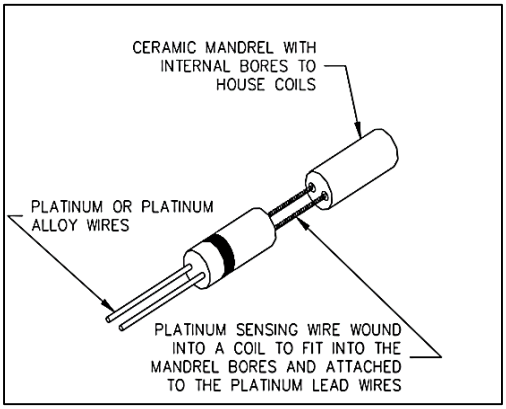

Figure 1-3 Wire Wound RTD [2]

Film type sensing elements are made from a metal coated substrate which has a resistance pattern cut into it. This pattern acts as a long, flat, skinny conductor, which provides the electrical resistance. Lead wires are bonded to the metal coated substrate and are held in place using a bead of epoxy or glass.

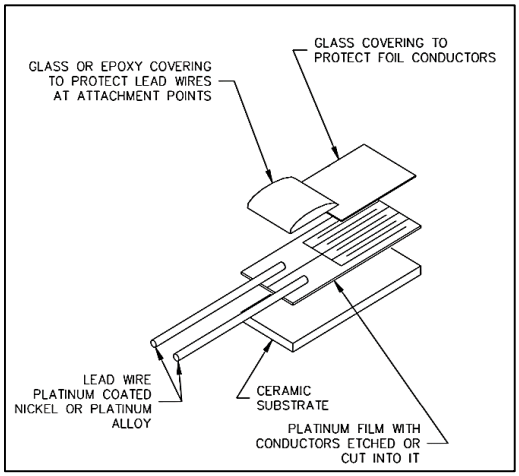

Figure 1-4 Thin Film RTD [2]

1.2.1 Indium Tin Oxide:

In this study, as explained, earlier an attempt has been made to use indium tin oxide as RTD element. Indium tin oxide (ITO, or tin-doped indium oxide) is a mixture of indium oxide (In_2O_3) and tin oxide (SnO_2), typically 90% In_2O_3, 10% SnO_2 by weight. When deposited as a thin film on glass or clear plastic it functions as a transparent electrical conductor. ITO has superior conductivity and transparency, stability and ease of patterning to form transparent circuitry. ITO is used in a number of display technologies, such as LCD, OLED, plasma, electroluminescent, and electro-chromatic displays, as well as in a number of touch screen technologies.

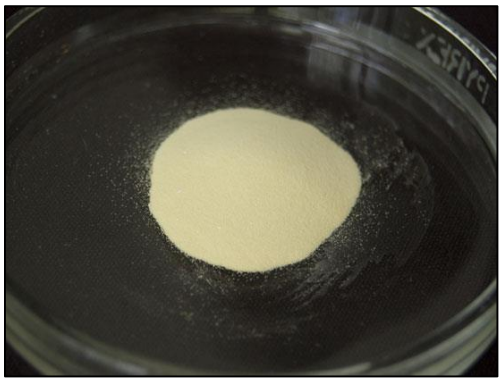

Figure 1-5 ITO in powder form [3]

Indium tin oxide coatings are used for antistatic coatings, EMI shielding, photovoltaic solar cells, aircraft windshields, and freezer case glass for demisting. ITO can be used as an infrared reflecting coating to reflect heat energy in Low-E glass and in low-pressure sodium lamps.

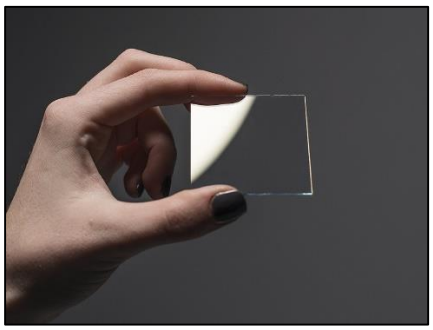

Figure 1-6 Thin Film ITO coated on glass [4]

It was observed that ITO thin film shows good linear resistance v/s temperature characteristic. Moreover, ITO has positive slope indicating that whenever there is an increase in temperature the resistivity of ITO thin film also increases. The thin film ITO resistor was designed keeping in mind the thermal and practical constraints of its usage in measuring the temperature of a hotspot in order to cool it with electrowetting on dielectric

technique(EWOD). Moreover, ITO is known for its ability to withstand harsh, oxidizing and nitride environments so it would act as a perfect sensing material for RTD fabrication. ITO is also a cost-effective choice of material when compared to platinum which is an advantage when fabricating a thin film RTD. The present study mainly focusses on fabricating, calibrating and characterizing the ITO RTD. In addition to that, repeatability of the ITO RTD was also checked. Annealing plays an important role in the changing the crystal structure of the oxide thin film. Effect of annealing on the resistivity was also studied by subjecting the thin film to high temperatures in air for the different amount of time.

1.2.2 Nickel:

For the comparison study, nickel was used in the fabrication of metal RTD. Being one of the most inert materials to many chemicals and having a linear positive resistance v/s temperature characteristic, nickel became a material of choice for designing a thin film RTD. Nickel is a cost-effective and easily available option. As a well-known fact, nickel also shows repeatability and is more accurate in measuring temperature over a limited range. Nickel is a good compromise between copper and platinum. Nickel was fabricated using similar microfabrication process as ITO and was annealed in the air before using it in experiments.

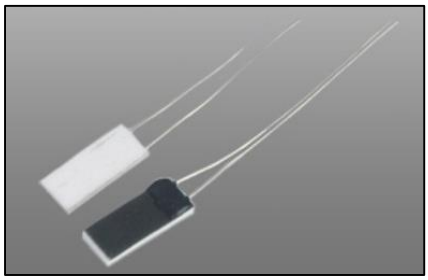

Figure 1-7 Thin Film Nickel RTD [5]

Chapter 2

LITERATURE REVIEW

Indium tin oxide thin films have very wide applications in day to day life because of its transparency and conductive nature. Research has been done to study the effect of heat treatment on various properties of ITO like resistivity, conductivity, optical transparency and its crystal structure to name a few. When ITO thin films are subjected to high temperatures, there is a significant change in its crystal structure. H. Morikawa et al. investigated the behavior of ITO films on the carbon substrate. They observed the structure of ITO thin films using transmission electron microscope(TEM). They observed that the film, when deposited by sputtering techniques, is almost amorphous in nature with a small amount of crystalline areas called nuclei. Most of these crystalline nuclei sites were generated directly on the substrate surface during deposition of ITO on the substrate. The nuclei gradually grow to keep the round shape with the increase in thickness, probably because of the temperature increase inevitably taking place during the deposition [6]. H. Morikawa and M. Fujita concluded in their research of crystallization of indium oxide(IO) and indium tin oxide thin films that the difference between ITO and IO thin films can be interpreted from the point of view that the dopant Sn supplies carriers in a crystalline ITO films but does not supply carriers in amorphous films. The carrier concentration in IO thin films did not increase with crystallization because it does not contain the dopant Sn [7]. On heat treatment at 513 K, the film was completely crystallized from its amorphous stage which resulted in the great decrease in resistivity value. Many carriers were released from crystallized areas of ITO [8]. S. Song et al. studied the thermal annealing of ITO films and concluded that as-deposited ITO film is amorphous structure. With the increase of temperature, the films show a polycrystalline cubic bixbyite In_2O_3 structure and also a drastic reduction in resistivity of ITO films [9]. Y. Shigesato and D.C. Paine in their study of

electronic properties of thin indium films concluded that dopant Sn remains inactive in the amorphous ITO and becomes active with crystallization. By examining hall mobility and carrier density at different temperatures they proved that Sn at high temperature provides free electrons along with oxygen atoms [10]. S. Muranaka et al. in their study of ITO thin films found that films (about 550 Å) were amorphous at room temperature, partially crystallized at 50–125°C and crystalline at 150–400°C [11]. J. Ederth et al. also found that both the charge carrier concentration and mobility increased upon annealing. The resistivity within the ITO nanoparticles was as low as $2^{x}10^{-4}$ Ω cm, which is comparable to the resistivity in dense ITO films made by physical vapor deposition [12]. After reviewing literature, the first set of experiments were carried out. It was found that ITO thin films after annealing at 200˚C. were still partially crystallized. The heating and cooling curve desired for RTD applications were not linear. The results have been discussed in the results and discussion section.

Paine et al. observed ITO thin film using TEM technique and found that as-deposited ITO film has a fully amorphous structure. After annealing in air at 162 °C, the sample becomes crystalline consisting of large block-like grains that are, on average, approximately 100 nm in size. The resistivity of the material changes because of relaxation of distorted bonds in the as-deposited amorphous material. Moreover, the experiments carried out on 180 nm thick ITO films showed that the resistivity becomes stable after keeping ITO films at high temperature for a considerably long amount of time [13]. T.J. Vink et al. also annealed ITO thin film to achieve crystallinity at 250˚C. By observing the microstructures under TEM it was found that The amorphous phase was always located at the substrate adjacent part of the film, and was crystallized by annealing. On the contrary, high-temperature films were homogeneously polycrystalline after deposition [14]. The experiments were then performed on new ITO RTD after increasing the time of annealing

up to 8 hours. The results are discussed in details in the results and discussion section. It was found that even though there was more linearity in heating and cooling cycle of ITO compared to previous experiments the desired RTD characteristics were still not found. There was also change in ITO base resistance value found in the multiple experiments that were carried out.

K.L Fang et al. also studied low-temperature crystallization of ITO thin films. They found that change in resistivity was very less when ITO was annealed at 150˚C compared to annealing at 180˚C. U. Betz et al. also carried out crystallization study of ITO thin films using SEM. They plotted resistivity vs temperature of ITO thin films and found that at 150 °C, the thermal activation induces the structural relaxation mechanism, resulting in an initial decrease of the resistivity value. No crystallization process occurred before 150˚C annealing temperature [15]. Moreover, the studies conducted by S. Song et al. and Y. Shigesato et al. also mentioned the fact that crystallization of ITO starts at 150˚C [9-10]. The possible reason behind this was the melting point of Indium which is 150˚C. Indium Corporation also mentioned that ITO showed stability in resistance value till 150˚C [16]. The decision was then taken to subject ITO under 150˚C. and carry out the experiments of RTD. The results are discussed in further sections.

ITO thin film resistance temperature detector characterization was carried out by Y. Wang et al. Their tests showed that resistance changed linearly with temperature and had a large value of temperature coefficient of resistance (TCR) at high temperatures [17]. The resistivity of ITO was checked by theoretical value [18].

The fabrication of nickel was also studied before carrying out the actual experiments. Arthur Chen et al. deposited a passivation layer on nickel layer before carrying out RTD experiments [19]. W.P. Yan et al. confirmed that glass is suitable as a substrate material for fabricating Nickel temperature sensor [20].

Chapter 3

EXPERIMENTAL DETAILS

3.1 DESIGN OF RTD:

The RTD design used for calibration purpose was taken from previous research carried out by Shreyas Bindiganavale et al [1]. The commercially available ITO on glass wafer were used for the experimental study. The thickness of glass substrate was measured by a laboratory micrometer screw having a thickness of 700 μm. The thickness of the ITO layer was measured by KLA Tencor Alpha-Step IQ profilometer of class 100 cleanroom of NanoFAB laboratory of The University of Texas at Arlington and it measured at 200 nm. Whereas the thickness of the nickel layer was also measured and it was having a thickness of 100 nm. The thickness of nickel layer was measured after the electron-beam deposition of nickel.

The resistance path of the RTD was made up of a serpentine pattern as shown in the figure. It was 620 μm ˣ 540 μm in overall dimension and had a width of 30 μm. The two large areas of 4000 μm ˣ 5708 μm are contact pads and are meant for external connections through copper wire. The copper wires were connected to the contact pads with the use of conducting epoxy and soldering. The copper plates were first attached to the contact pads by using a conducting epoxy. The copper wires were soldered on the copper plates by the normal soldering process. The entire connection was sealed by a non-conductive epoxy to ensure that the connection does not break away at high temperature.

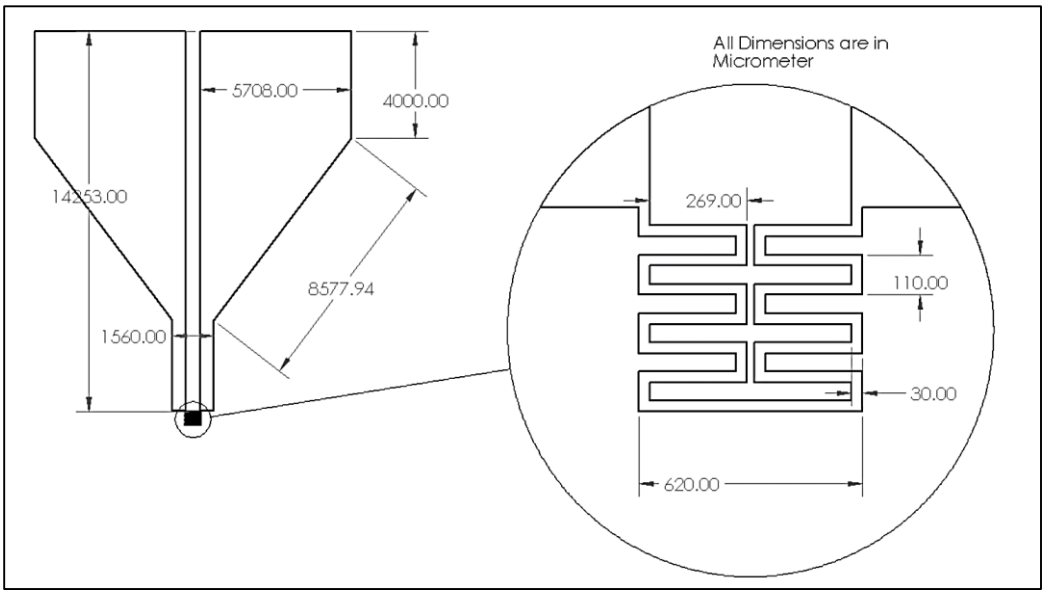

Figure 3-1 Design of RTD and its magnified view

3.2 EXPERIMENTAL SETUP DETAILS:

For the calibration of RTD, an experimental setup was designed and fabricated as shown in the schematic diagram below. Oil bath calibration technique was employed in this study. As shown in the figure, the RTD/Heater to be calibrated was dipped in an oil bath. The oil was utilized to ensure uniform steady state temperature condition over the entire surface of RTD material. The oil used here was Valvoline SAE 0W-20. The oil is contained in a glass wool insulated borosilicate glass container/beaker. In order to increase the temperature of oil for calibration purposes, a laboratory hot plate of Fisher Scientific

ISOTEMP was utilized. For maintaining uniformity and for reducing the time of reaching steady state temperature, constant stirring of the oil was carried out by a magnetic stirrer.

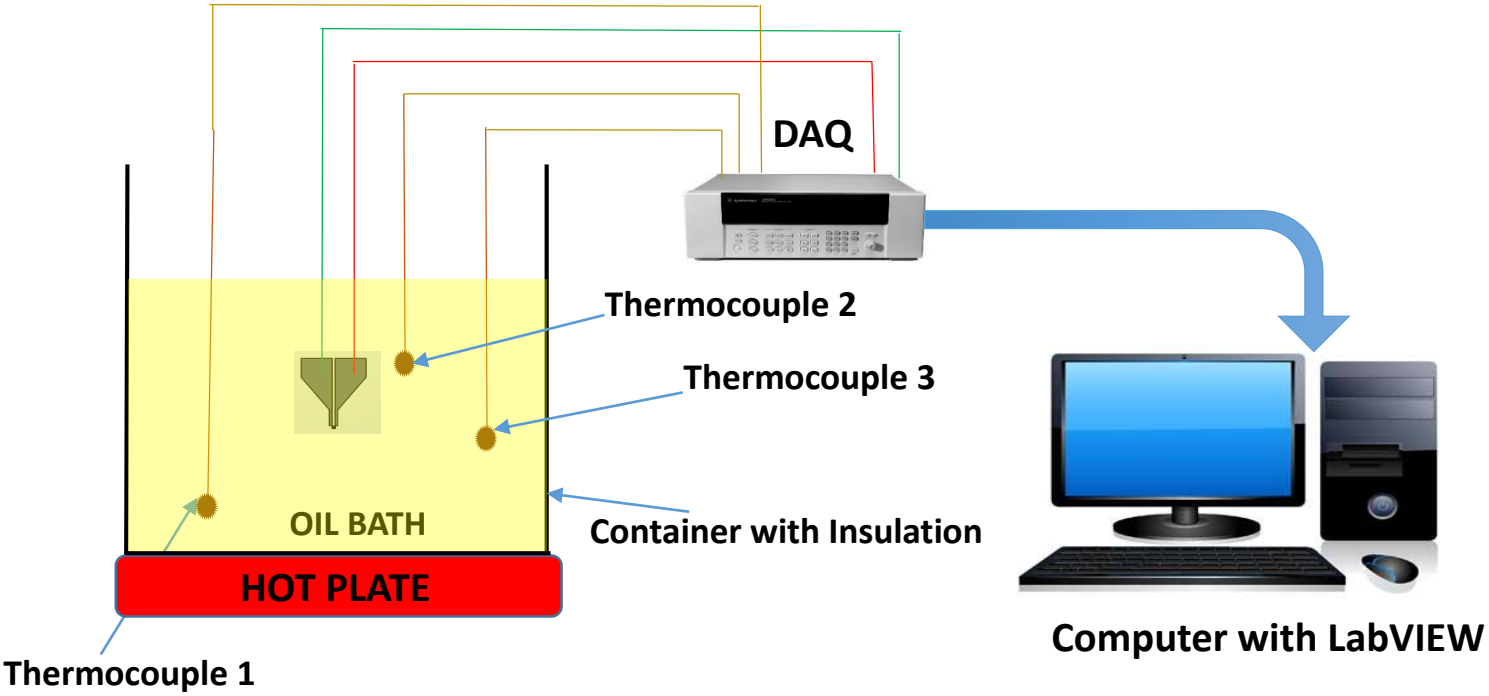

Figure 3-2 Schematic of Experimental Setup

The temperature of oil was measured by dipping three thermocouples in it. The thermocouples used were laboratory insulated thermocouple of “K” type and “J” type. These thermocouples were arranged in different locations in the oil bath. One was located near the hot plate, the second one was located near the RTD and the third one was held near the top surface of the oil. These type of arrangement of thermocouples at different locations ensured uniformity in temperature at all points of the oil bath and also a steady state temperature which is highly recommended for calibration readings.

Figure 3-3 Data Acquisition System Agilent 34980A

The thermocouples and RTD connections were connected to different channels on the back side of Agilent 34980A Data Acquisition System. The Data Acquisition (DAQ) System is used for the measurement, control, and activation of thermocouples and RTD. The DAQ uses 4-wire resistance measurement technique for measuring the resistance of the RTD. It sends an electric current in μ-amp through one channel and measures the voltage through other. The thermocouples were connected at different channels for the measurements.

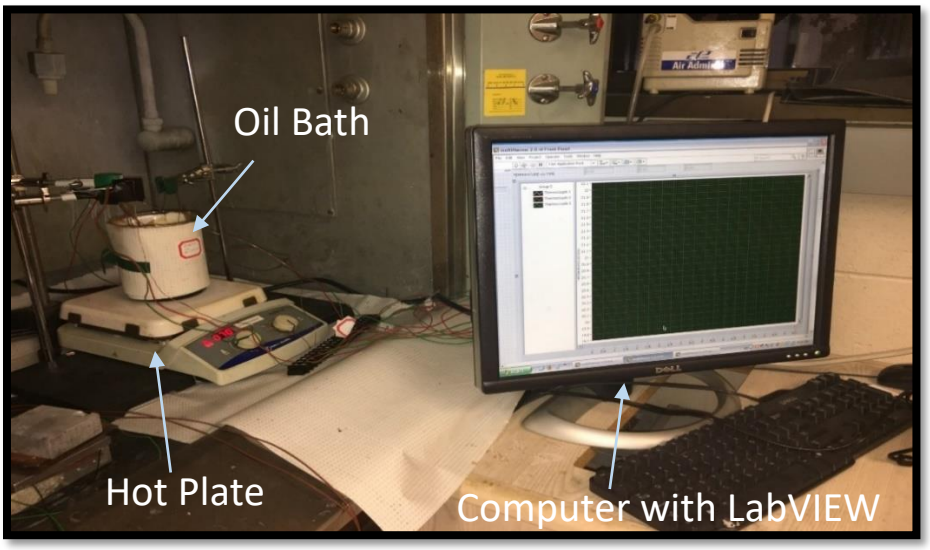

Figure 3-4 Experimental Setup

The data acquisition was monitored by LabVIEW software through a personal computer system. NI LabVIEW 2015 was used for monitoring entire experimental setup. The NI LabVIEW is a system design platform and development program for a visual programming language. It is used for data acquisition, instrument control and industrial automation on a variety of operating systems. The LabVIEW program was developed according to the arrangement of instruments attached in DAQ and was meant for continuous measurement using a timed loop.

3.3 Mask Design:

As mentioned in the design of RTD section the RTD/Heater devices were fabricated using standard microfabrication methods with facilities UTA NanoFab. Figure “3-5” shows the mask used for RTD fabrication.

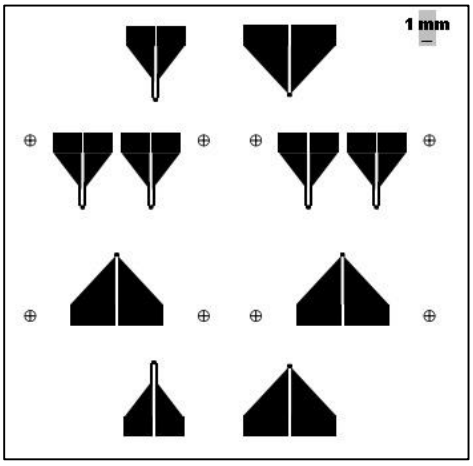

Figure 3-5 Mask showing design of RTD device [1]

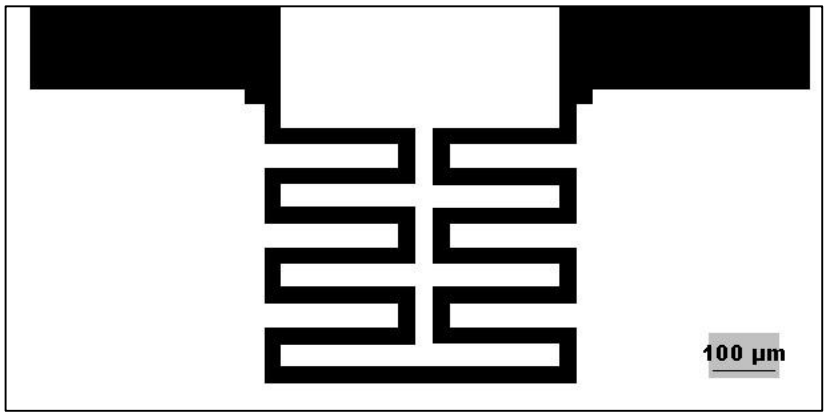

Figure 3-6 Magnified View of RTD design [1]

The mask for RTD was designed using L-Edit software by Tanner EDA. The final circuit design was exported to GDS (Graphic Data System) file type and was then converted to PostScript (PS) format using Link CAD software. The PostScript format helps us to view the final design which was similar to PDF format. The PS file was sent to a mask printing company, CAD/Art Services Inc., Oregon. These masks were used in the photolithography process.

3.4 Fabrication process:

3.4.1 Fabrication of ITO Resistive Temperature Detector:

The fabrication of Indium Tin Oxide RTD was carried out in Class 100 cleanroom of NanoFab laboratory of The University of Texas at Arlington. The fabrication includes cleanroom MEMS microfabrication processes which are: spin coating, photolithography, developing, wet etching, a photoresist (PR) stripping and baking. A four-inch ITO wafer on a glass substrate was used for RTD fabrication. Before carrying out the fabrication process, a thorough cleaning of a wafer was done with the help of acetone, isopropyl alcohol and methanol as cleaning agents. Furthermore, deionized (DI) water was used for rinsing the

wafer. After rinsing, the wafer was blow dried with nitrogen gas and dehydrated on a hot plate (Isotemp, Fisher Scientific) at 150 °C. Spin coating is a process of deposition of thin films of uniform thickness on a substrate by spinning the substrate with the thin film material over it. Hexamethyldisilazane (HMDS), a colorless solution, was spin coated prior to spin coating of photoresist (PR) over the wafer for the purpose of better adhesion of PR to an ITO wafer. HMDS was carefully poured on a wafer and spun using a custom made recipe. This recipe involved spinning the wafer to 500 rpm for the first 5 seconds and then ramping it up to 4000 rpm at a rate for 900 rpm/s. The wafer was spun for the next 30 seconds at a constant speed. After spin coating of HMDS, the wafer was soft baked at 110 °C for 1.5 min. According to the mask design, a positive PR named S1813 was used in this fabrication. The same recipe which was used for spin coating HMDS was also used for spin coating PR. It was followed by a soft bake at 115 °C for 60 seconds. After the spin coating process, UV exposure was done. The fabrication process flow is shown in Figure 3-7.

Photolithography is used to remove selective parts of PR. A lithography mask (Figure 3-5) is used in this process. An ITO wafer spin-coated by HMDS and PR is subjected to high energy UV exposure for 8 seconds. UV light passes through the blank area on the mask and does not pass through the printed black portion. This changes the chemical properties of PR (sensitive to light) which affects only the blank area through which it passes. A post exposure bake was done at 115 °C for one minute to harden the PR which is left on the wafer. After this stage, developer solution (MF-319) was used to dissolve and remove part of the PR which was exposed to UV rays, this left behind the unexposed PR which formed the pattern.

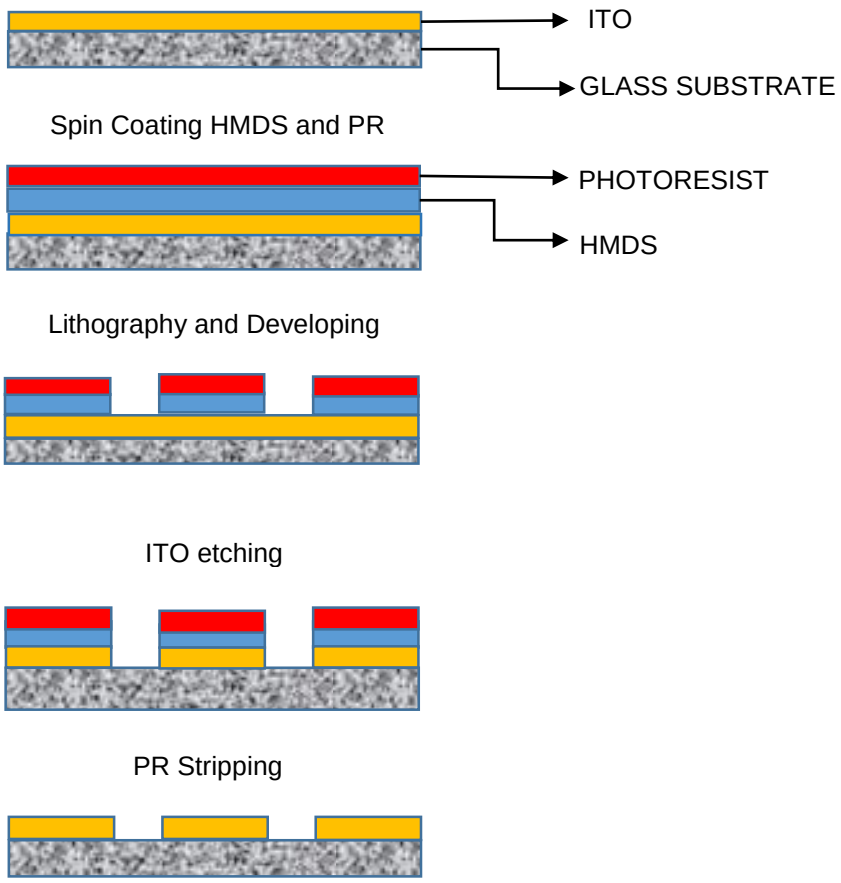

Figure 3-7 Steps showing ITO fabrication process

A post developing bake was carried out before etching, so that, etching does not affect the PR layer. An etchant solution comprised of HNO3, HCl and DI water in proportion, 1:8:15 was used. The etchant was heated up to 55 °C. This process was carried out for 5 mins. Lastly, a PR stripper solution was used to remove the baked PR to expose the chip with ITO patterned heater. ITO RTD was then ready to calibrate in the oil bath.

3.4.2 Fabrication of Nickel Resistive Temperature Detector:

The fabrication of nickel RTD was carried out in Class 100 cleanroom of NanoFAB laboratory of The University of Texas at Arlington. The fabrication includes cleanroom MEMS microfabrication processes which are: E-Beam deposition, spin coating, photolithography, developing, wet etching, the photoresist (PR) stripping and baking.

A four-inch plain glass substrate was used for RTD fabrication. Nickel was deposited on the glass wafer using E-beam evaporator. Prior to the fabrication process, a thorough cleaning of a wafer was done with the help of piranha solution as cleaning agents. Piranha solution is a mixture of Sulfuric acid (H_2SO_4) and Hydrogen peroxide (H_2O_2),it is used to clean organic residues off glass surface. Piranha Solution has a ratio of sulfuric acid to hydrogen peroxide as 3:1. This makes the surface of glass perfectly cleansed having no amount of impurities on it which makes it suitable for nickel to deposit and bond with the glass surface. Deionized (DI) water was used for rinsing the wafer after the Piranha Solution cleaning. After rinsing, the wafer was blow dried with nitrogen gas and dehydrated on a hot plate (Isotemp, Fisher Scientific) at 150 °C. Hexamethyldisilazane (HMDS), a colorless solution, was spin coated prior to spin coating of PR over the wafer for the purpose of better adhesion of PR to an ITO wafer. HMDS was carefully poured on a wafer and spun using a custom made recipe which is similar to that used in ITO RTD fabrication. According to the mask design, a positive PR named S1813 was used in this fabrication. The same recipe which was used for spin coating HMDS was also used for spin coating PR. It was followed by a soft bake at 115 °C for 60 seconds. After spin coating process, UV exposure was done. The fabrication process flow is shown in Figure 3-8

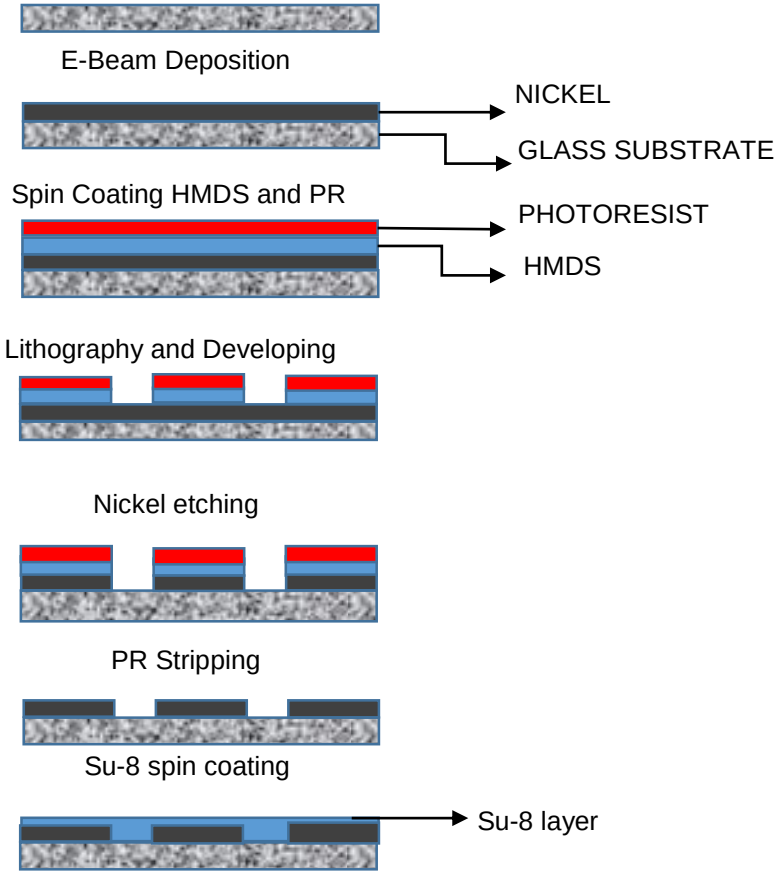

Figure 3-8 Steps showing Nickel fabrication process

Photolithography and developing of Nickel is done in the same way as that of ITO by exposing it for 8 seconds and carrying out developing with MF-319 as a developer. A post developing bake was carried out before etching, so that, etching does not affect the PR layer. Nickel etchant was used in etching of Nickel from the exposed part. It is typical a mixture of HNO_3 and H_2O in the ratio of 1:13. The wafer was dipped in the etchant solution for 50 seconds at room temperature. Lastly, a PR stripper solution was used to remove the baked PR to expose the chip with nickel patterned RTD.

3.5 LABVIEW SETUP:

Laboratory Virtual Instrument Engineering Workbench commonly known as LabVIEW is a design platform/environment for a visual programming language from National Instruments [22]. It is a graphical design platform wherein users can create a flow diagram to perform any type of mathematical, control system, measurement, and data acquisition operation. LabVIEW is commonly used for instrument control, automation, data acquisition, and embedded control systems. LabVIEW is beneficial for interfacing the devices, code compiling and parallel programming.

It integrates the creation of user interfaces into a development cycle. The subroutine programs in LabVIEW are called virtual instruments (VIs). Each VI has a front panel, block diagram/Back Panel and a control palette. The front panel is the user interface VI which has the input and output control, indicators, graphs and numerical data to display [22]. A control palette is a component which contains the controls and indicators used to create the front panel. It can be accessed from the front panel window by selecting "View" and then "Controls Palette" from the top menu of the front panel window or by right clicking on the empty space in the front panel. A Block diagram/Back Panel contains the functions and graphical source code. The wiring and actual modeling of a program are done in the block diagram panel which is the actual graphical programming screen.

3.5.1 Flowchart for LabVIEW setup:

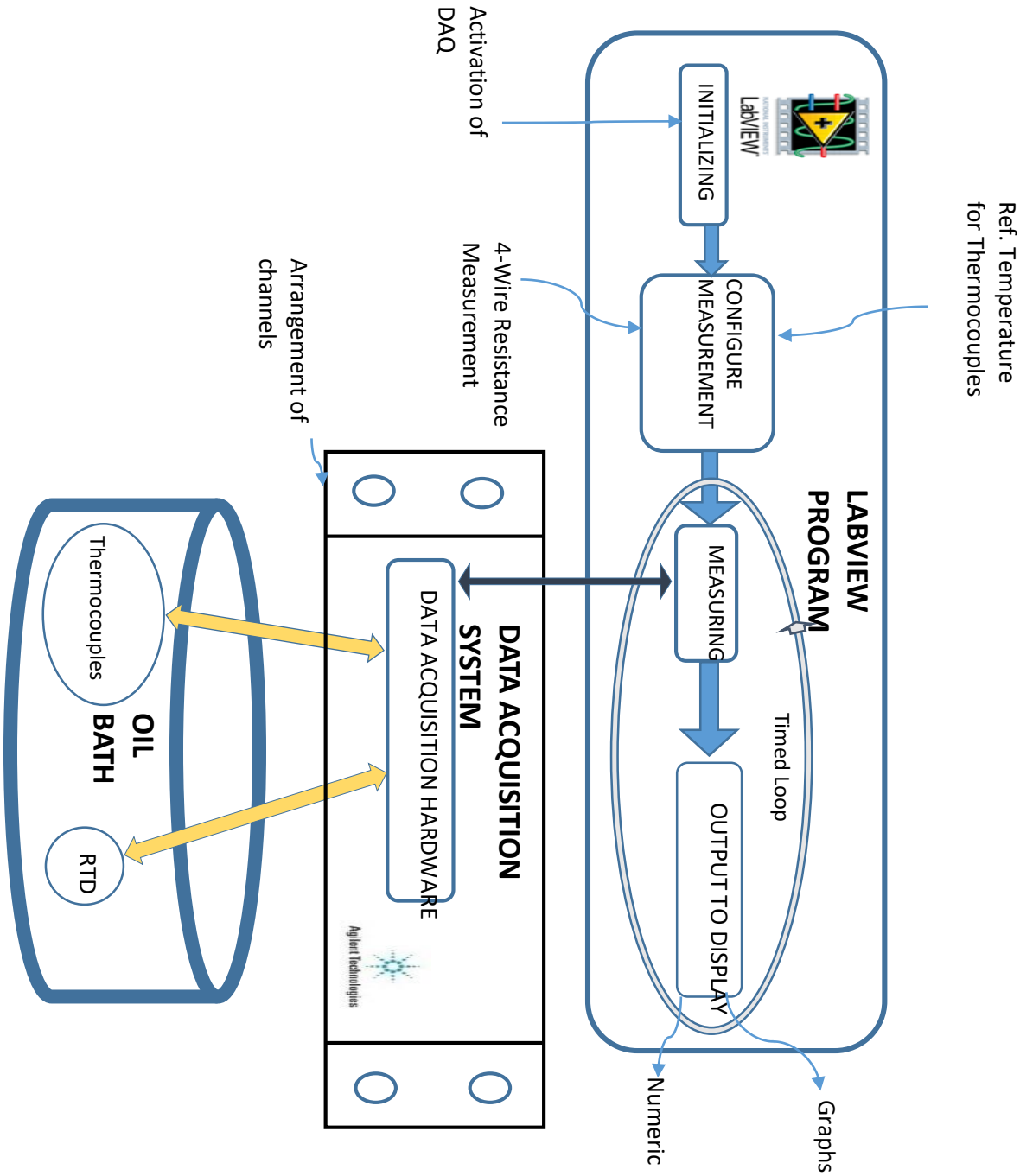

Figure 3-9 Flowchart for LabVIEW Setup

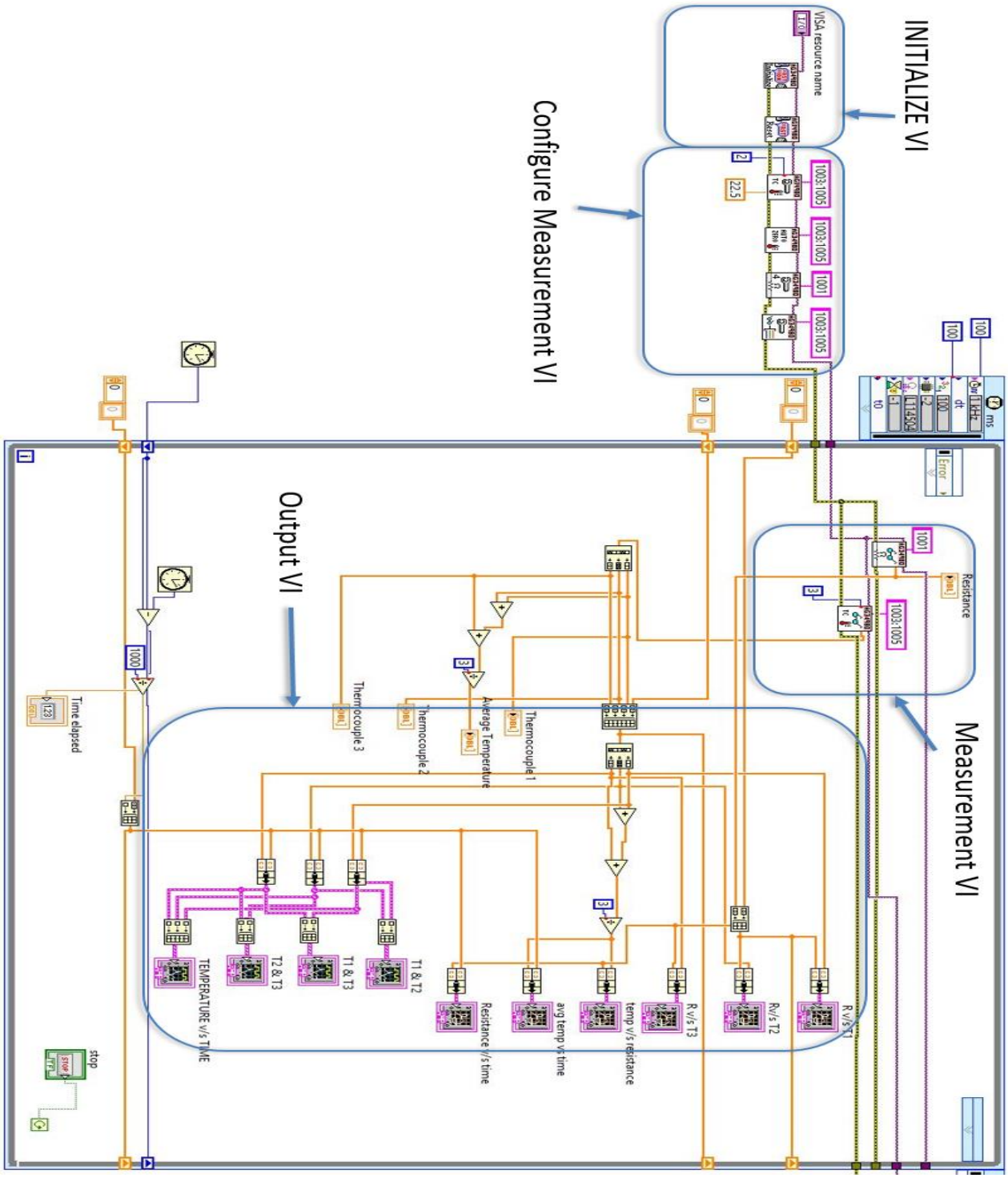

Figure 3-10 LabVIEW Setup

The basic flowchart of all the programming in LabVIEW is as shown in figure 3-9 and the actual LabVIEW program is shown in figure 3-10. Here specific set of similar subroutines or VIs are clubbed together and shown as one block diagram. The “Initializing VIs” initializes the program as well as the DAQ and the channels for the thermocouples and RTD connected to it. The actual activation of DAQ is done through initializing VIs. The DAQ resource name or address is assigned in VI called “VISA Resource name” by the user in the front panel. “Initialize AG34980” initializes the DAQ i.e. Agilent 34980A.In the “Configure Measurement” VIs, all the thermocouples and the RTD which are connected to the DAQ are called in the LabVIEW program. It sets the arrangement of the measurement of thermocouples and RTD according to the cycle by scanning it in DAQ. Moreover, the assignment of reference temperature (22˚C) to the thermocouples, the type of thermocouple used (i.e. “J” type) and the method of resistance measurement of the RTD is carried out by “Configure Measurement” VIs. The DAQ uses 4-wire measurement by sending current through one set of channels and measuring voltage through other set of channels.

Timed loop is used for continuous measurements necessary for calibration purposes. It is used to execute sub diagrams or frames sequentially in the order which is defined by the user. It is used to take continuous measurements from the thermocouples and RTD that are connected to DAQ. The period between two consecutive measurement readings and the sequence of measurement is carried out by the timed loop. Initially a time of 100 ms is given for the “Measurement” VIs after it is scanned by the “Scan” VI in previous step. The time given between two consecutive measurements or readings is 100 ms. This time gap is decided according to the VI’s used and more most accurate measurement readings.

Inside the timed Loop, “Measurement VI” and “Output VIs” are connected. “Measurement TC” is used to take continuous readings from all the thermocouples dipped in oil bath. “Measurement Resistance(Ω)” is used to take continuous readings from the RTD to be calibrated. These VIs are the one which are directly connected to the Agilent DAQ system. The measuring VIs displays output also. These outputs are arranged in a sequential manner using number of arrays provided by LabVIEW. The split arrays and the build arrays have been utilized here. The data coming from “Measurement TC” VI is split into three sub-data. This enables the user to know continuous temperature readings of the three thermocouples separately ensuring all the temperature readings are consistent and similar all the time during steady state condition.

The “Build Array” function is also used to display the data in graphical manner. In a similar manner, resistance data is also being displayed on the front panel. The “Output VIs” are the ones which displays output in front panel in a graphical as well as numerical manner. The graphs displayed on the front panel are of “Resistance vs Time”, “Temperature vs Time”, “Resistance vs Temperature” and “Avg. Temperature vs Time”. The time taken on the ordinate of the graphs is the exact time of the cycle in seconds. The machine clock VI is taken inside the timed loop as well as outside the timed loop. The difference in the two clocks is evaluated which gives the exact time of the cycle. All the data is then clubbed together using array function and is displayed in “X-Y Graph” VI from control palette. The numeric displays of temperatures, resistance and time is taken from measuring VI and displayed on the front panel.

The thermocouples and RTD measurement is taken from data acquisition system. This DAQ system assign channel numbers to each device that are being connected to it. The number basically starts from 1000.There are 64 channels in the multiplexer of the system. Each thermocouple is connected to one set of channel, whereas resistance

measurement of RTD is carried out using two set of channels. According to the measurement technique, which is 4-wire resistance measurement, the current is supplied to the RTD from 1 set of channel in micro-amp range and the other set of channel measures the voltage readings across the contact pads of RTD. The ratio of voltage to current gives the value of resistance of the RTD.

Copper wires are used for the connection purposes of thermocouples and RTD which are attached to the channels of the multiplexer of DAQ system.

3.6 OIL Bath Calibration:

Figure 3-12 Oil Bath [23]

Figure 3-11 Valvoline 0w-20 [24]

As we have seen in the experimental setup of RTD Calibration, motor oil was used as a medium to maintain uniform temperature. The oil bath calibration technique was chosen because it can maintain steady state temperature necessary for calibration. It maintains uniformity of temperature on entire surface of RTD. In addition to that, the temperature of oil can be controlled with ease by the hot plate which is an advantage over the use of laboratory ovens. Moreover, many oils are inert to the material of devices so there is very less chances of reaction of oil with the material in contact.

As mentioned before, motor oil of Valvoline brand having grade “SAE-0W-20” was used for the experiment. The boiling point of motor oil is 300˚C which is relatively high. Moreover, the flash point of this motor oil is 240˚C which indicates that there will be no breakage of synthetic compounds found in oil below this temperature. This temperature range satisfies the need of calibration. The thermal time constant (τ) of motor oil was also calculated using the formula:

$\tau = ((\rho * c_p * V)/(h * A))$

where ρ = density, c_p = specific heat and V = body volume,

h=heat transfer coefficient and

A=Total surface area

Here an assumption of heat transfer coefficient of oil was made as 50W/(m^2•K) in low convection condition. The specific heat was taken as c_p =2.8 kJ/(Kg-K) and the density of layer of ITO was taken as ρ=7140 kg/m^3. The calculations of the area and volume were carried from the design of RTD section.

The value for thermal time constant for ITO layer = 0.06 s whereas that of Nickel layer=0.0058 s.

As the thermal time constant value is very less, this indicates that the time required for the oil to reach steady state was very less and so motor oil was a preferred choice for the calibration of RTD.

3.7 Experimental Procedure:

As explained in the experimental setup, the experiment is started when we turn on the LabVIEW program and also increase the temperature of oil bath using the hot plate. The thermocouples and RTD which are dipped in oil bath are connected to DAQ and starts taking the readings as per the LabVIEW program. The oil is constantly stirred to maintain uniformity of temperature. The readings are plotted in the “X-Y plot” VI of LabVIEW. The temperature of the oil bath was increased by the hotplate to a specific pre-determined value. When the temperature of all the three thermocouples reaches at that value, the readings of the RTD was noted. The numeric as well as graphical data of the front panel helps us to know the exact temperature and resistance. The oil bath was maintained at that specific temperature for a considerable amount of time after which the temperature was increased up to next specific value. This cycle was repeated number of times until the maximum value of temperature was reached and was termed as heating cycle. After the maximum temperature is attained, the “Cooling cycle” was plotted. The temperature of oil was allowed to cool up to next similar specific temperature as used in “Heating cycle”. Here the readings of RTD was taken in the same manner by maintaining the steady state for considerable amount of time thereby plotting the cooling curve of the cycle. Utmost care was taken in maintaining steady state of the oil bath. Entire experiment was carried out keeping the setup under exhaust fan. The graph which was plotted was then taken in MATLAB figure and were displayed for analysis.

Chapter 4

RESULTS AND DISCUSSION

The major focus of conducting tests were to verify the results of research work done in the effect of heat treatment on ITO thin films. After studying the change in crystal structure because of heat treatment on ITO, the similar tests were conducted on one sample of ITO RTD on glass substrate. The ITO sample was annealed for 2 hours at 200˚C temperature in air inside the heating oven. After annealing, the sample was subjected to multiple tests in the same manner as discussed in experimental procedure section. The results were plotted using MATLAB tool as shown in Figure 4-1.

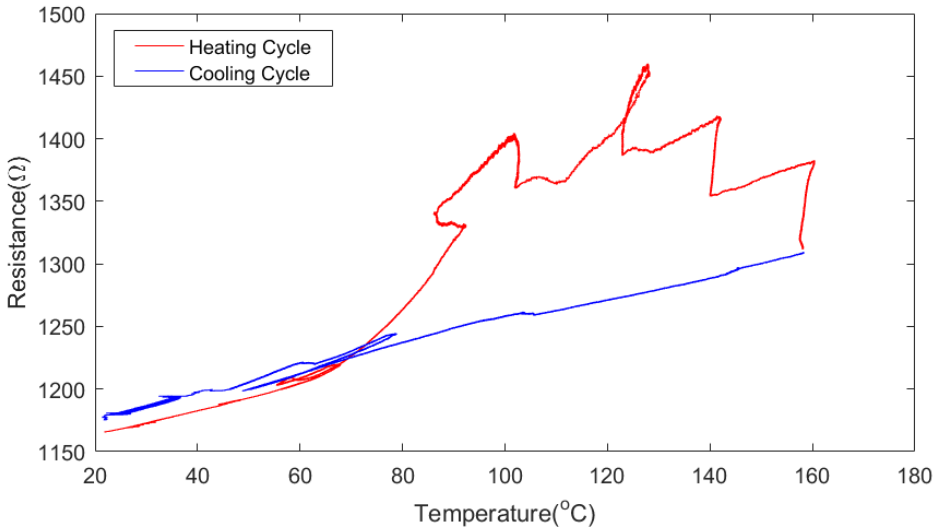

Figure 4-1 Test 1 on ITO sample 1

As seen from the figure there was a decrease in Resistivity of ITO thin film at high temperature as observed by the heating cycle curve. The sample was subjected to maximum temperature of 155˚C in the oil bath and then cooled down. To check the repeatability of the results multiple tests were carried out on the same sample and the graphs were plotted as shown in figure 4-2,4-3,4-4.

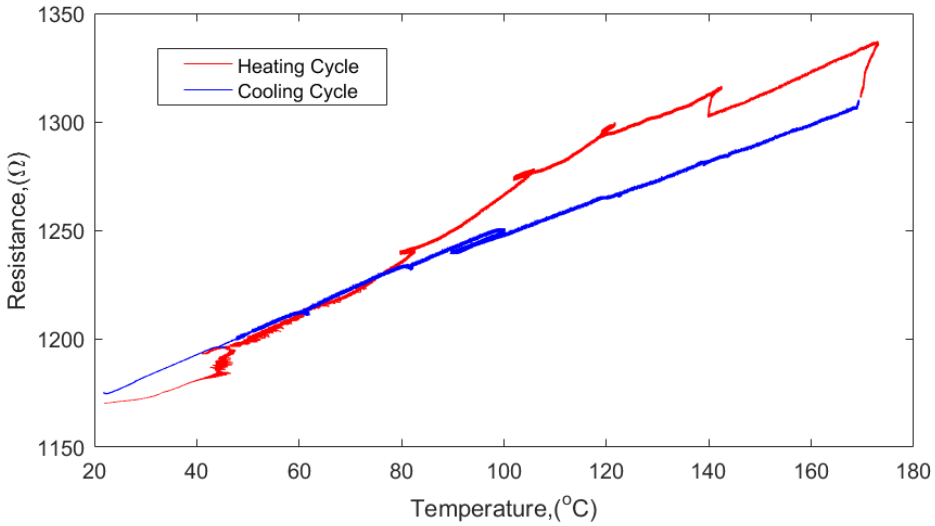

Figure 4-2 Test 3 on ITO RTD sample 1

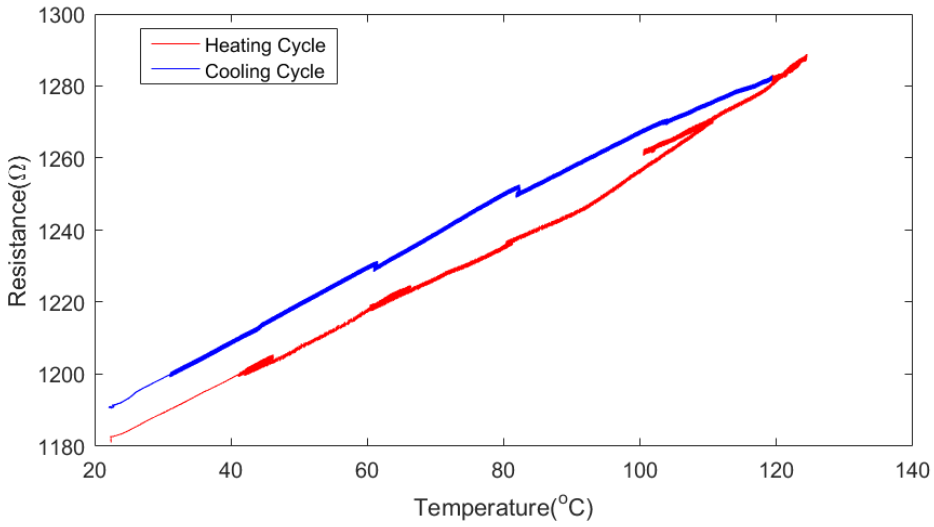

Figure 4-3 Test 6 on ITO RTD sample 1

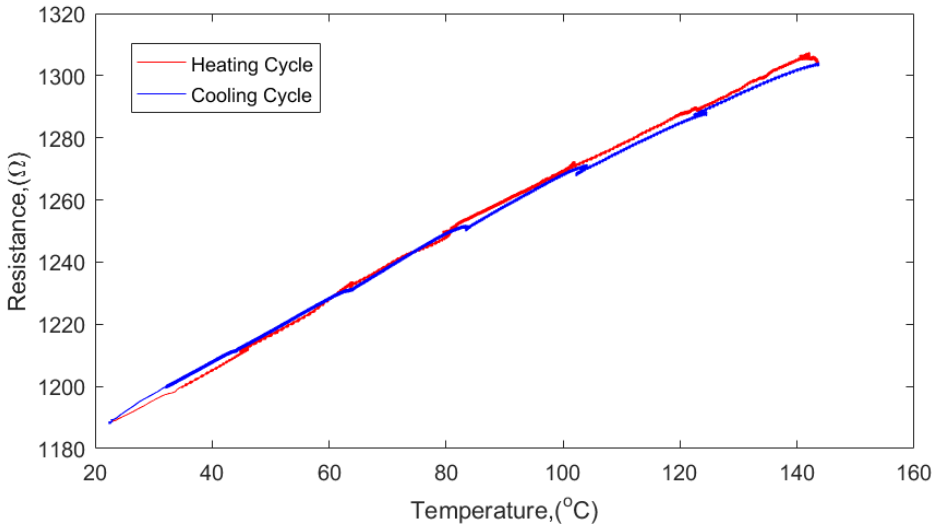

Figure 4-4 Test 8 on ITO RTD sample 1

The tests were carried out by first heating the ITO sample from room temperature to a high temperature (typically between 120˚C to 175˚C) and after that cooling the sample up to room temperature. The sample was kept at steady state temperature at certain pre-determined temperature values while heating and cooling. As seen from Figure 4-2, 4-3 and 4-4, it was concluded that ITO sample showed non-linear resistance v/s temperature characteristics. The drop in resistance at high temperature and change in base resistance (resistance at room temperature) indicates that there was partial crystallization of ITO thin film. As the ITO RTD was first annealed at 200˚C and then was subjected to multiple tests, so the crystallization temperature of ITO which was found from research literature to be 150˚C. was crossed but was not completed so it was only partially crystallized. After conducting multiple tests, it was also concluded that there was no repeatability of ITO RTD sample. At last, the results concluded that annealing at high temperature for two hours does not give satisfying results and this ITO sample cannot be used for RTD purposes. In addition to that, as seen from Figure 4-4, the multiple tests also helped in partial crystallization of the ITO structure and that may be the reason behind the more linear

nature of resistance v/s temperature curve in Test 8 compared to previous tests. The linear nature here indicates that the heating cycle and cooling cycle of RTD fell on the same curve on R v/s T graph.

The partial crystallization of ITO thin film proves the results of H. Morikawa et. al in his study of thin film ITO crystallization as explained in the literature review section.

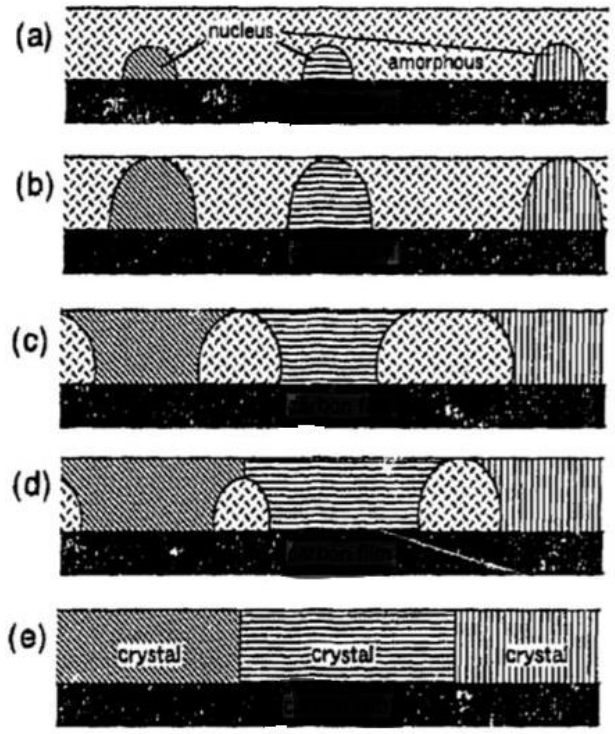

Figure 4-5 Crystallization of ITO thin film [8]

The literature study was again carried out after first set of experiments and results obtained from the experiments inferred that the time of Annealing of the ITO sample should be increased. This may help in full crystallization of ITO thin film after which it could be used as temperature sensing device. As explained by Paine et. al in his research work, the

resistivity of ITO thin film, as shown in Figure 4-6, reduces and remains almost steady after annealing at high temperature for 8 hours.

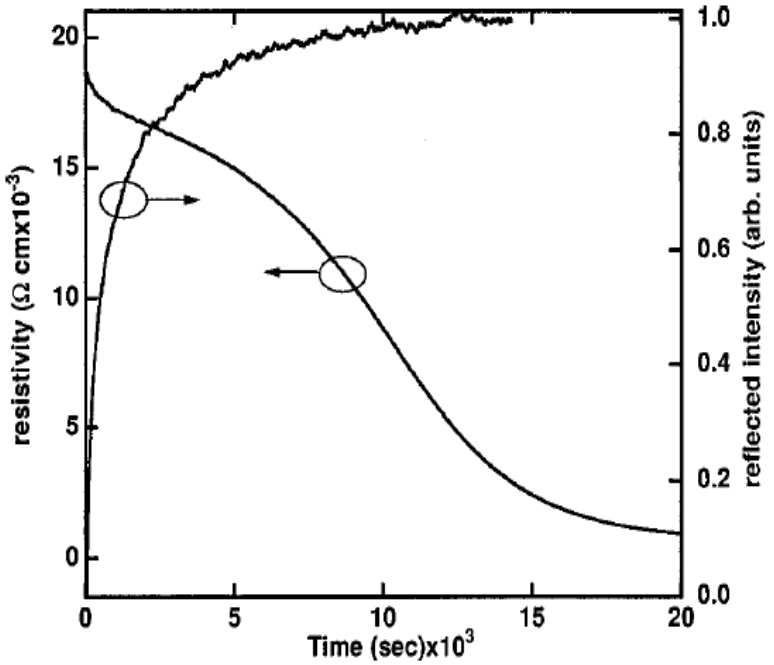

Figure 4-6 Resistivity change with time [14]

Also the resistivity of the material changes because of relaxation of distorted bonds in the as-deposited amorphous ITO material. After reviewing the literature, the decision was taken to increase the time of annealing up to 8 hours keeping the temperature similar to the previous sets of experiments. The results obtained were as shown in figures 4-7,4-8,4-9,4-10.

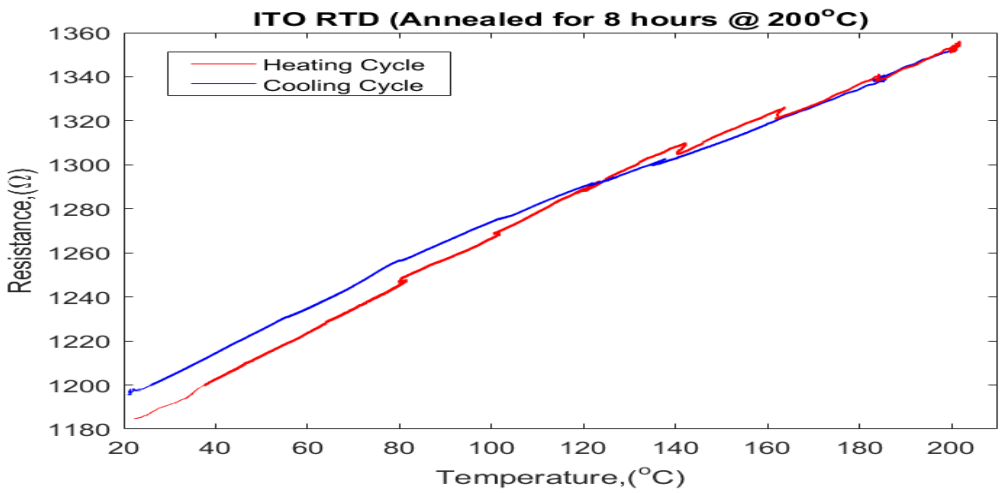

Figure 4-7 Test 1 on ITO RTD sample 2

As seen above, the ITO sample showed more linear temperature v/s resistance characteristics. Multiple tests were carried out and the results were plotted as shown in figure 4-8,4-9 and 4-10.

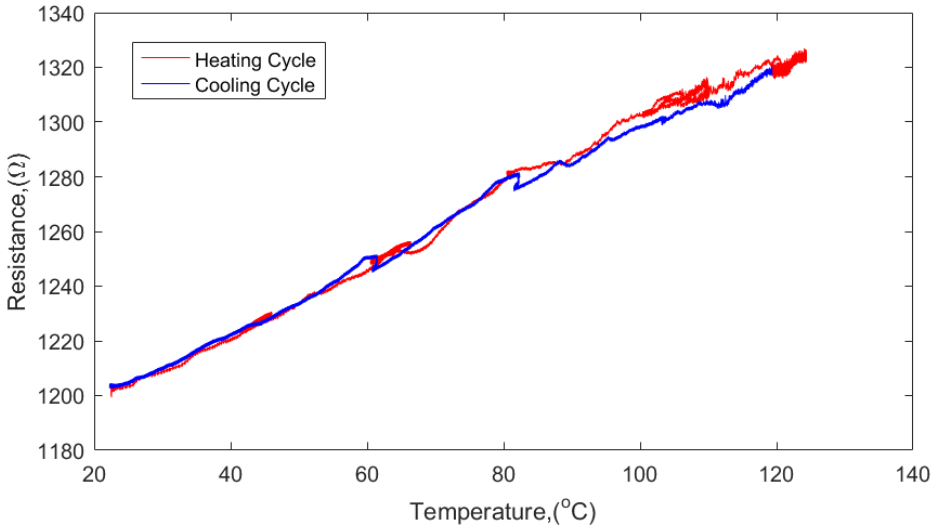

Figure 4-8 Test 2 on ITO RTD sample 2

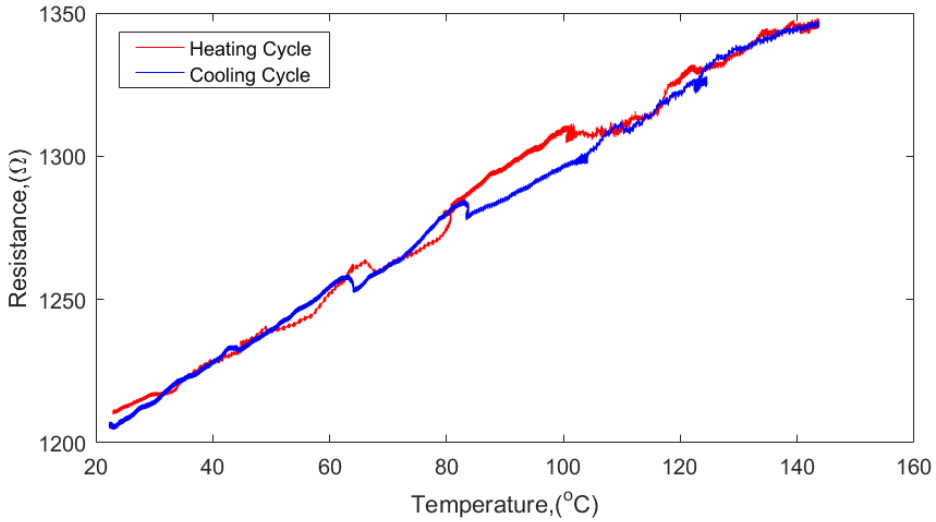

Figure 4-9 Test 3 on ITO RTD sample 2

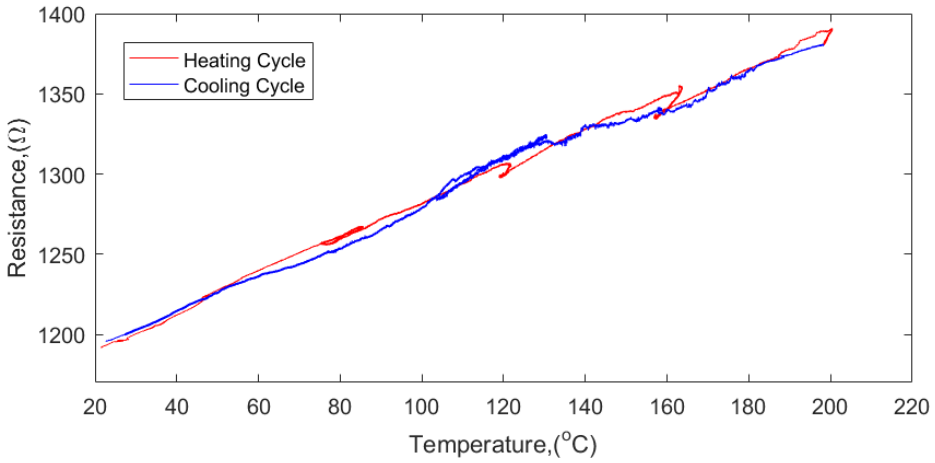

Figure 4-10 Test 4 on ITO RTD sample 2

The experiments highlighted the fact that although the decrease in resistance was lesser compared to first tests, there was still a change observed in the value of base resistance (at 22° C) after the sample is heated up and cooled down. Moreover, the

calibration curve was also not linear as required for RTD. Multiple tests still resulted in non-repeatability of results. All the experiments carried out proved the fact that increase in annealing time does not fully crystallize the ITO sample.

After reviewing the research work carried out by K.L. Fang et al. and also from U. Betz et al as discussed in literature review section, the crystallization of ITO starts at around 150˚C. The resistivity change does not start before this temperature value. So it was decided that instead of crystallizing the ITO sample, if it subjected to temperature not higher than 150˚C, the linear curve that is required for resistance thermometer can be achievable. The third test were carried out without annealing the sample and also by keeping the temperature range below 150˚C. The results obtained are as shown in Figure 4-11 and Figure 4-12.

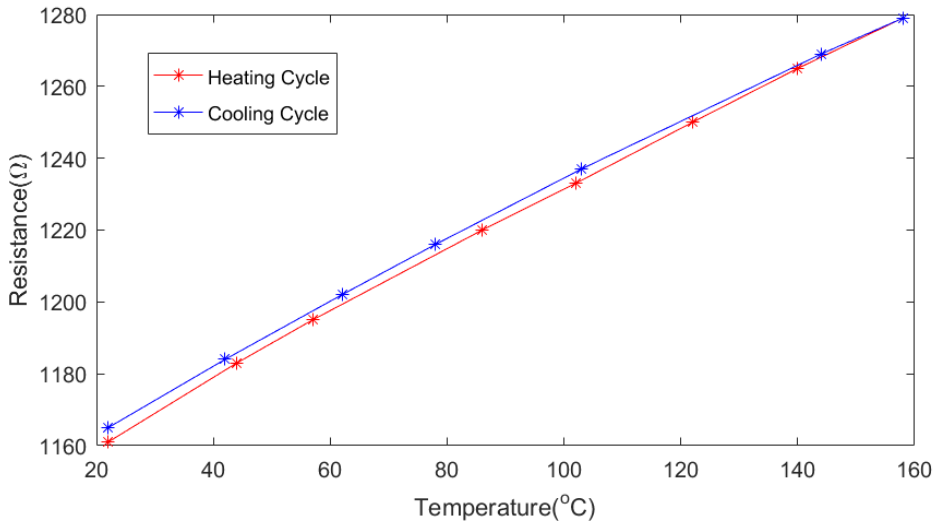

Figure 4-11 Test 1 on ITO RTD sample 3

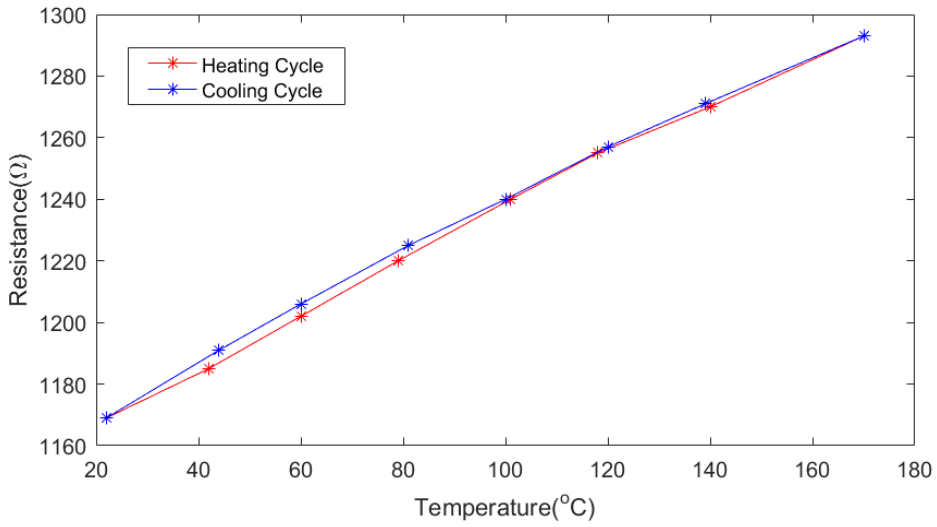

Figure 4-12 Test 3 on ITO RTD sample 3

In the third experiment carried out on ITO sample, the sample was subjected to temperature slightly higher than 150˚C which is crystallization temperature of ITO. Multiple tests were carried out on the same sample. The results clearly indicate that ITO sample shows near linear positive temperature v/s resistance characteristics with no change in base or reference resistance value. Multiple tests also prove the repeatability of the data. The results from the tests were combined and were plotted on one single graph (Figure 4-13) which showed us the error bar also. There is an error of 1˚C in all the readings.

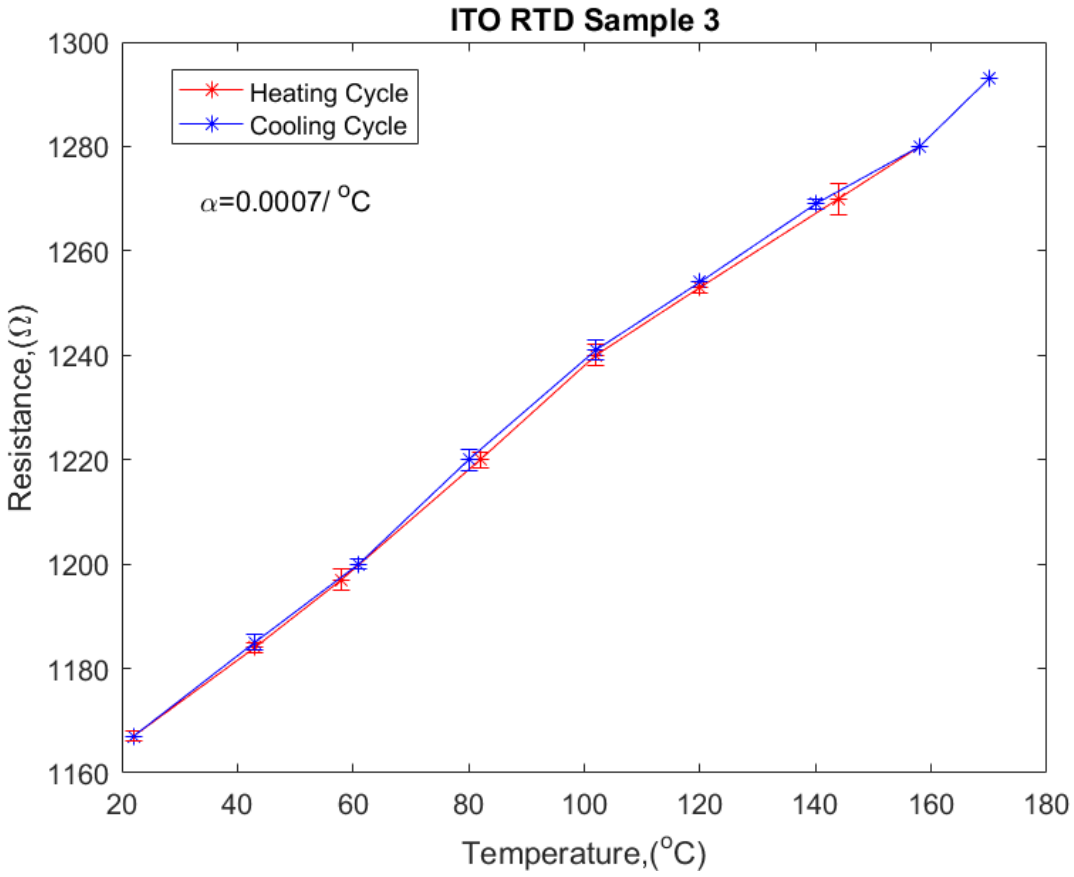

Figure 4-13 Average of four tests on ITO RTD sample 3

It can be interpreted from the above graph that the ITO sample when subjected to temperature lower than 150˚C ,which is crystallization temperature of ITO, shows positive Temperature v/s Resistance Characteristics with TCR value of 0.0007 /˚C. Moreover, the heating and cooling curve also follows the same path and it is also repeatable. Experiment was also conducted on ITO sample which was subjected to temperature lower than 150˚C to prove the repeatability and consistency of the data. The results were plotted as shown in figure 4-14 and figure 4-15.

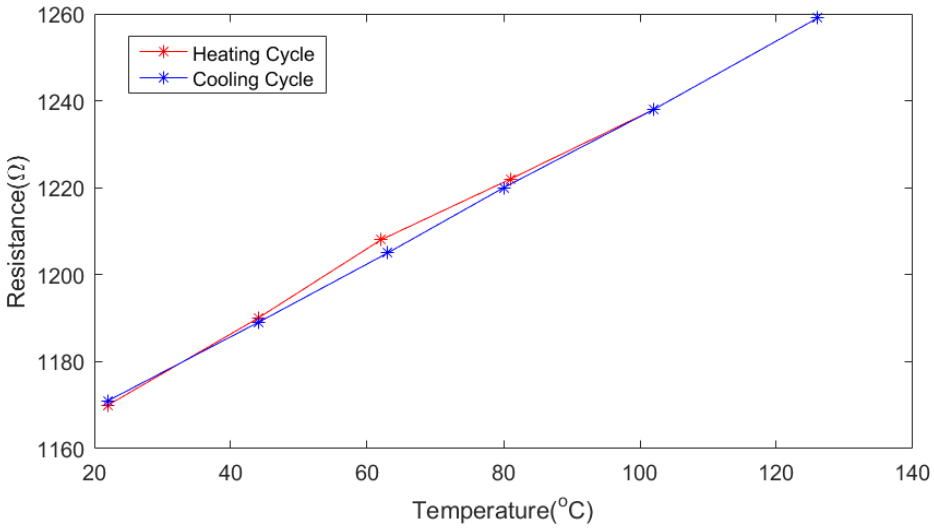

Figure 4-14 Test 1 on ITO RTD sample 4

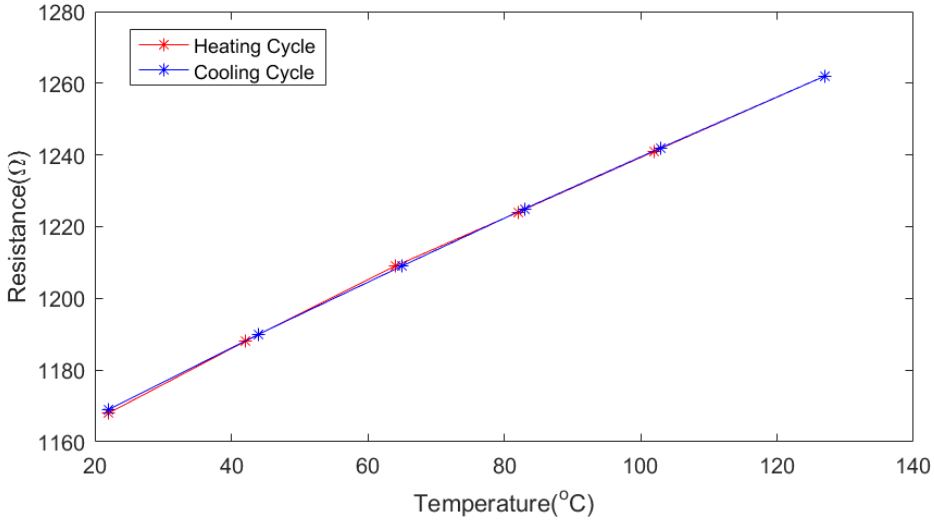

Figure 4-15 Test 2 on ITO RTD sample 4

From the graph, it can be proved that ITO, when subjected to temperature lower than 150˚C, shows almost linear positive temperature v/s Resistance characteristics. Multiple tests proved the repeatability of the data. The value of TCR was calculated and it was 0.0007 /˚C. The data from all four tests were put together and were plotted on one graph as shown in figure 4-16.

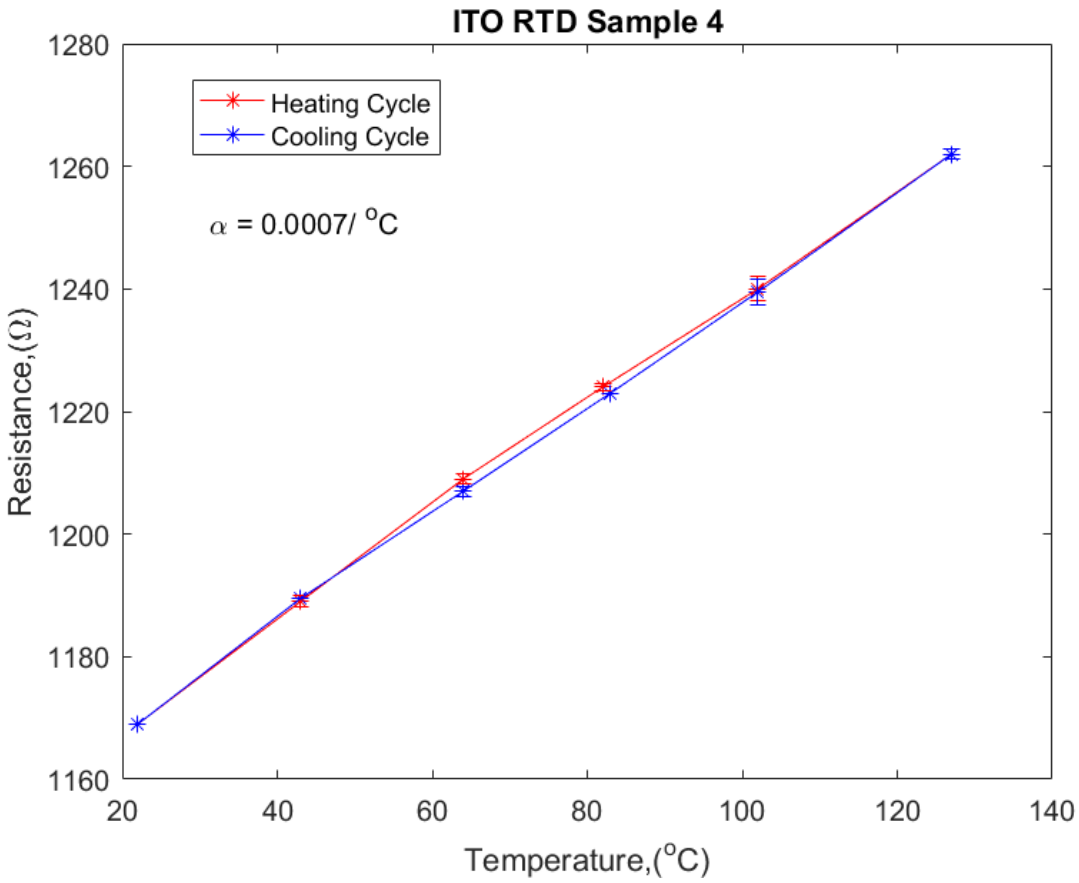

Figure 4-16 Average of three tests on ITO RTD sample 4

The value of resistivity of the sample was measured by VEECO FPP-5000 4-Point Probe and it came out to be 2.3×10^{-4} Ω-cm.

On the other hand, nickel was also calibrated for high temperature applications. Nickel RTD which were fabricated in clean room were tested with the same experimental procedure. The nickel sample was annealed at 200˚C for 2 hours. Three tests were carried out and the results were plotted as shown in Figure 4-17.

The nickel RTD showed linear positive temperature v/s resistance characteristics for higher temperature range (22˚C to 200˚C). In addition to that, multiple tests also showed repeatability of the RTD. Moreover, there were no changes observed in the value of base resistance value of nickel RTD. Hence it was concluded that nickel sample can be utilized for higher temperature range. The graphs were combined in one single figure and plotted as shown in Figure 4-17.

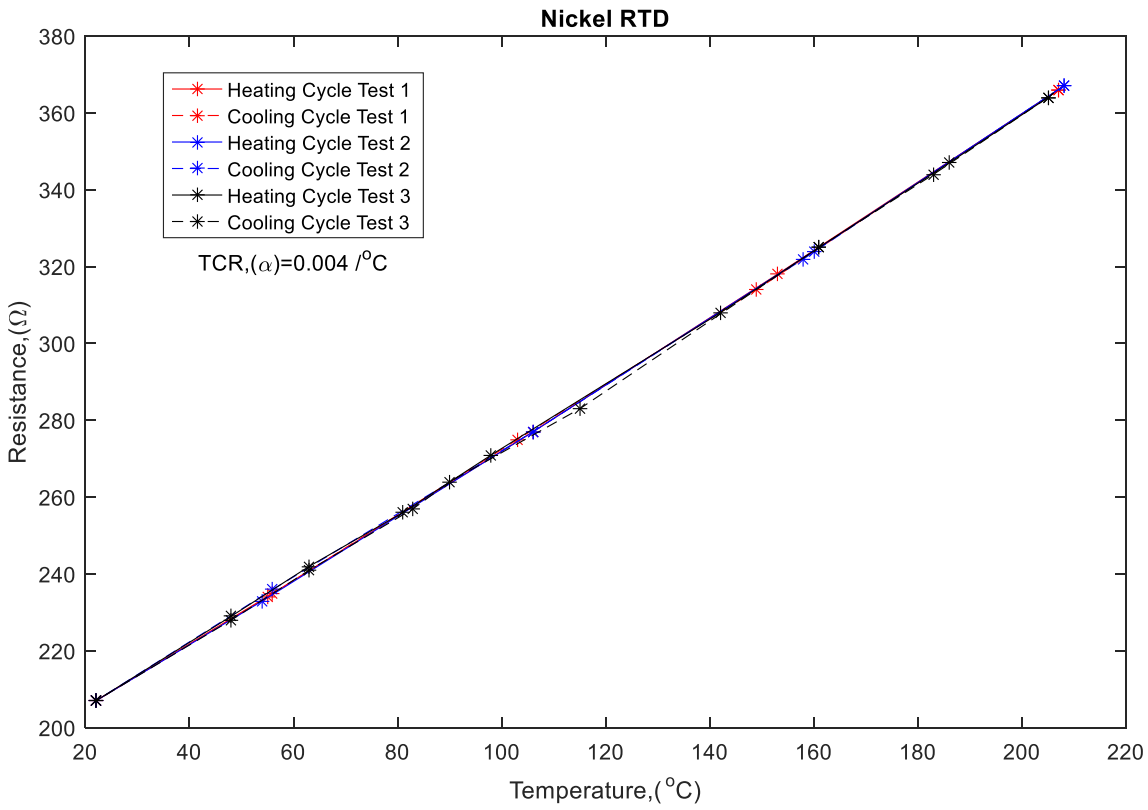

Figure 4-17 Nickel RTD Sample

The value of temperature co-efficient of resistivity for nickel sample were calculated to be 0.004 /˚C which was in good agreement with the theoretical value as explained in literature review section. The value of resistivity was also measured by VEECO FPP-5000 4-Point probe which came out to be 6.11×10^{-6} Ω-cm.

4.1 RESULT TABLE

Table 1:Result Table

	Annealing Conditions	Samples of RTD	Operating Temperature	Nature of Plot	Repeatable	Resistivity(ρ)(in Ω-cm)	TCR (/˚C)
ITO	2 Hours @ 200˚C	Sample 1	22˚C-150˚C	Non-linear	No	2.3×10^{-4}	N/A
	8 Hours @ 200˚C	Sample 2	22˚C-150˚C	Non-linear	No	2.3×10^{-4}	N/A
	Non-annealed	Sample 3	22˚C-150˚C	Linear	Yes	2.3×10^{-4}	0.0007
		Sample 4					
Nickel	2 Hours @ 200˚C	Sample 1,2,3	22˚C-200˚C	Linear	Yes	6.11×10^{-6}	0.004

Chapter 5

CONCLUSION AND FUTURE SCOPE

5.1 Conclusion

The experimental work and literature research were carried out for the fabrication, calibration and characterization of micro-scale resistive temperature detector for measuring temperature at micro-scale level. From this study, it was concluded that:

1. Experimental results prove that indium tin oxide, a transparent semi-conductor, can be used as resistive temperature detector in the temperature below 150˚C.
2. The ITO thin film changes its state from amorphous to polycrystalline when subjected to high temperature (above 150˚C).
3. Annealing plays an important role in changing the state of indium tin oxide from amorphous to polycrystalline.
4. Experimental results prove that nickel when coated with a passivation layer can be used as RTD in the temperature range of 22˚C-200˚C.

5.2 Future Scope

In future the study of the behavior of ITO thin film with different deposition techniques Like magnetron sputtering, Ion-Beam sputtering, Sol-gel method and Evaporation method can be carried out.

Research in calibration of ITO thin film for very high temperature applications is being done and ITO can be a very stable material at high temperatures [22].

References

[1] S. Bindiganavale, "Study of Hotspot Cooling for Integrated Circuits Using Electrowetting on Dielectric Digital Microfluidics," no. May, 2015", Ph.D, The University of Texas at Arlington, 2015.

[2] http://archives.sensorsmag.com/articles/0101/24/main.shtml

[3] http://www.indium.com/inorganic-compounds/indium-compounds/indium-tin-oxide/

[4] https://cdn-shop.adafruit.com/1200x900/1310-00.jpg

[5] https://www.heraeus.com/us/group/products_and_solutions_group/
sensor technology/sensor products/sensors.aspx

[6] Hiroshi Morikawa, Haruhiko Sumi, Masayoshi Kohyama, "*Crystal growth of ITO films prepared by DC magnetron sputtering on C film",* Thin Solid Films 281-282 (1996) 202-205.

[7] Morikawa, H Fujita, M, "*Crystallization and Electrical Property Change on the Annealing of Amorphous Indium Oxide and Indium-Tin Oxide Thin Films",* Thin Solid Films 359 (2000) 61-67.

[8] Morikawa, H Fujita, M, *"Crystallization and decrease in resistivity on heat treatment of amorphous indium tin oxide thin films prepared by d.c. magnetron sputtering",*Thin Solid Films 339 (1999) 309-313.

[9] Song Shumei,Yang Tianlin, Liu Jingjing, Xin Yanqing, Li Yanhui, Han Shenghao, *"Rapid thermal annealing of ITO films",* Applied Surface Science 257 (2011) 16 7061-7064.

[10] Shigesato, Yuzo Paine, David C, *"Study of the effect of Sn doping on the electronic transport properties of thin film indium oxide"*, Applied Physics Letters 62, 1268 (1993); doi: 10.1063/1.108703.

[11] S. Muranaka, Y. Bando, T. Takada, *"Influence of substrate temperature and film thickness on the structure of reactively evaporated In_2O_3 films",* Thin Solid Films 151 (1987) 335.

[12] J. Ederth, Johnson P., G. A. Niklasson, A. Hoel, A. Hultaker, P. Heszler, C. G. Granqvist, A. R. van Doorn, M. J. Jongerius, D. Burgard, *"Electrical and optical properties of thin films consisting of tin-doped indium oxide nanoparticles",* Physical Review B 68 155410 (2003).

[13] Paine David C, Whitson T, Janiac D, Beresford R, Yang Cleva Ow, Lewis Brian, *"V A study of low temperature crystallization of amorphous thin film indium – tin – oxide A study of low temperature crystallization of amorphous thin film indium – tin – oxide*", J. Appl. Phys., Vol. 85, No. 12, 15 June 1999.

[14] T.J. Vink, W. Walravae, J.F.C. Daams, P.C. Baarslag and J.E.A.M. Meerakker: On “the homogeneity of sputter-deposited ITO films. Part I: Stress and microstructure”. Thin Solid Films 266, 145 (1995).

[15] Betz U., Olsson, M Kharrazi, Marthy J., Escolá M F, Atamny F, “Thin films engineering of indium tin oxide: Large area flat panel displays application”, Surface & Coatings Technology 200 (2006) 5751–5759.

[16] Indium Corporation*, “Indium Oxide and Indium-Tim Oxide (ITO) Coatings”,86 (2013)*

[17] Wang Yanlei, Zhang Congchun, Li Juan, Ding, Guifu Duan, Li, *“Fabrication and characterization of ITO thin fi lm resistance temperature detector”, Y. Wang et al. / Vacuum xxx (2016) 1e5.*

[18] Chapter 2 Indium-Tin Oxide: Its Preparation, Properties and Characterization.

[19] Arthur C.M. Che and James M. Lommel, “*Thin Film Nickel Temperature Sensor*”,3748174 July-1973.

[20] Weiping Yan, Henan Li, Yongbian Kuang, Liquan Du, Jihong Huo*, “Nickel membrane temperature sensor in micro-flow measurement.”* Journal of Alloys and Compounds 449 (2008) 210-213.

[21] Wang Yanlei, Zhang Congchun, Li Juan, Ding Guifu, Duan Li, *“Fabrication and characterization of ITO thin film resistance temperature detector”* Vacuum xxx (2016) 1-5.

Biographical Information

Kunjan Anilkumar Chaudhari was born in Vadodara, Gujarat, INDIA in 1990. He received his Bachelor of Engineering degree from The Maharaja Sayajirao University of Baroda, India, in 2013. He joined The University of Texas at Arlington (UTA) in 2015. He is currently a member of Integrated Micro-Nano fluidic systems laboratory at UTA. His research interest lies in Digital Microfluidics, Thermal Engineering ,MEMS fabrication and Data Acquisition using LabVIEW.